NATO Science Fellowship Programme by the Scientific and Technical Research Council of Turkey and also the financial support of the Technical University of Denmark Department of Energy Engineering and Department of Mechanical Engineering. Thanks are also owed to Knud Erik Meyer for his expert assistance in LDA measurements.

References

[1]Fric, T. F., and Roshko, A., "Vortical Structure in the Wake of a Transverse Jet," *Journal of Fluid Mechanics*, Vol. 279, 1994, pp. 1–47.

[2]Kelso, R. M., Lim, T. T., and Perry, A. E., "An Experimental Study of Round Jets in Cross Flow," *Journal of Fluid Mechanics*, Vol. 306, 1996, pp. 111–144.

[3]Yuan, L. L., Street, R. L., and Ferziger, J. H., "Large-Eddy Simulations of a Round Jet in Crossflow," *Journal of Fluid Mechanics*, Vol. 379, 1999, pp. 71–104.

[4]Kim, K. C., Kim, S. K., and Yoon, S. Y., "PIV Measurements of the Flow and Turbulent Characteristics of a Round Jet in Crossflow," *Journal of Visualization*, Vol. 3, No. 2, 2000, pp. 157–164.

[5]Özcan, O., and Larsen, P. S., "An Experimental Study of a Turbulent Jet in Cross-flow by Using LDA," Dept. of Mechanical Engineering, Technical Univ. of Denmark, Rept. MEK-FM 2001-02, Lyngby, June 2001.

[6]Yuan, L. L., and Street, R. L., "Trajectory and Entrainment of a Round Jet in Crossflow," *Physics of Fluids*, Vol. 10, No. 9, 1998, pp. 2323–2335.

[7]Tobak, M., and Peake, D. J., "Topology of Three-Dimensional Separated Flows," *Annual Review of Fluid Mechanics*, Vol. 14, 1982, pp. 61–85.

[8]Perry, A. E., and Chong, M. S., "A Description of Eddying Motions and Flow Patterns Using Critical-Point Concept," *Annual Review of Fluid Mechanics*, Vol. 19, 1987, pp. 125–155.

[9]Meyer, K. E., Özcan, O., and Westergaard, C. H., "Flow Mapping of a Jet in Cross-flow with Stereoscopic PIV," *Journal of Visualization*, Vol. 5, No. 3, 2002, pp. 225–231.

[10]Lim, T. T., New, T. H., and Luo, S. C., "On the Development of Large-Scale Structures of a Jet Normal to a Cross Flow," *Physics of Fluids*, Vol. 13, No. 3, 2001, pp. 770–775.

R. M. C. So
Associate Editor

Test Data Uncertainty Analysis Algorithm of NASA Ames Wind Tunnels

Norbert M. Ulbrich*
Sverdrup Technology, Inc.,
Moffett Field, California 94035-1000

Nomenclature

B = systematic uncertainty
$\boldsymbol{B}$ = systematic uncertainty vector
B' = correlated systematic uncertainty
b_k = systematic uncertainty of an elemental error source
e_i = component of the unit precision uncertainty vector
$\boldsymbol{e}_i$ = unit precision uncertainty vector
e_k = component of the unit systematic uncertainty vector
$\boldsymbol{e}_k$ = unit systematic uncertainty vector
i = index of a measured variable
j = index of a measured variable
k = index of an elemental error source
M = total number of elemental error sources
N = total number of measured variables
P = precision uncertainty
$\boldsymbol{P}$ = precision uncertainty vector
p_i = component of the precision uncertainty vector
R_i = range of a measured variable
r = result
U = total uncertainty
x_i = measured variable
Δx = step size used for the numerical differentiation
δ_{ij} = Kronecker delta
ε = relative machine precision
λ = characteristic scale
μ = index of a measured variable
ξ = index of an elemental error source

Received 23 February 2002; revision received 16 September 2002; accepted for publication 3 March 2003.

*Senior Aerodynamicist. Member AIAA.

Introduction

A TEST data uncertainty analysis system is being developed for NASA Ames wind tunnels. After reviewing some of the available literature on uncertainty analysis,[1–3] it was decided to implement Meyn's[3] uncertainty propagation methodology in the uncertainty analysis system. His methodology is mathematically identical with the traditional methodology that is recommended in the AIAA Standard[1] on wind-tunnel test data uncertainty analysis. Meyn's approach, however, makes complex uncertainty correlations between measurements easier to understand as no covariance matrix is needed.

In the first part of this Technical Note, a new derivation of Meyn's uncertainty propagation law is presented. Then, it is shown how Meyn's vector approach can be extended to precision uncertainty estimates. Issues related to the numerical calculation of partial derivatives are also discussed. Finally, key elements of the proposed uncertainty analysis algorithm are summarized.

Estimate of Uncertainty

In most practical applications a result is given by a data reduction equation of the type

$$r = r(x_1, \ldots, x_N) \tag{1}$$

where $x_1, \ldots, x_N$ are measured variables. The square of the total uncertainty of the result equals the sum of the squares of the systematic and precision uncertainties. Then, we get[2]

$$U^2(r) = B^2(r) + P^2(r) \tag{2}$$

where $B(r)$ is the systematic uncertainty and $P(r)$ is the precision uncertainty of the result.

Systematic Uncertainty

In general, using the traditional uncertainty analysis methodology, the systematic uncertainty $B(r)$ of a result is given by the following formula[2]:

$$B(r) = \sqrt{\sum_{i=1}^{N}\left(\frac{\partial r}{\partial x_i}\right)^2 B^2(x_i) + 2\sum_{i=1}^{N-1}\sum_{j=i+1}^{N}\frac{\partial r}{\partial x_i}\frac{\partial r}{\partial x_j}B'(x_i, x_j)} \tag{3a}$$

$$B^2(x_i) = \sum_{k=1}^{M} b_k^2(x_i) \tag{3b}$$

$$B'(x_i, x_j) = \sum_{k=1}^{M} b_k(x_i) b_k(x_j) \tag{3c}$$

where the systematic uncertainty $B(x_i)$ and the correlated systematic uncertainty $B'(x_i, x_j)$ of a measured variable x_i are a function of uncertainties $b_k(x_i)$ of elemental error sources.

Coleman and Steele[2] define variable M in Eqs. (3b) and (3c) as the number of elemental error sources that are common for measured variables x_i and x_j. However, Eq. (3a) still remains valid if a more general definition of M is used. Variable M can also be defined as the total number of elemental error sources of all measured variables $x_1, \ldots, x_N$ assuming that uncertainty $b_k(x_i)$ equals zero if x_i is independent of elemental error source k.

In a recent paper Meyn[3] introduced a new uncertainty propagation methodology that can be applied to the calculation of systematic uncertainties. His methodology is mathematically identical with the traditional methodology. However, it greatly simplifies the investigation of systematic uncertainties as no covariance matrix is needed.

Meyn uses a vector approach to modeling uncertainty propagation. His uncertainty propagation law can be derived from the traditional uncertainty methodology by rewriting Eq. (3a) in a form that uses the Kronecker delta. The Kronecker delta is defined as

$$\delta_{ij} = \begin{cases} 1 & \text{if} \quad i = j \\ 0 & \text{if} \quad i \neq j \end{cases} \tag{4}$$

Then, we get for the square of Eq. (3a) the expression [see Ref. 1, Eq. (2–A–15)]

$$B^2(r) = \sum_{i=1}^{N} \left(\frac{\partial r}{\partial x_i} \right)^2 B^2(x_i) + \sum_{i=1}^{N} \sum_{j=1}^{N} (1 - \delta_{ij}) \frac{\partial r}{\partial x_i} \frac{\partial r}{\partial x_j} B'(x_i, x_j) \tag{5}$$

Combining Eqs. (3b) and (3c) with Eq. (5), we get

$$B^2(r) = \sum_{i=1}^{N} \left(\frac{\partial r}{\partial x_i} \right)^2 \sum_{k=1}^{M} b_k^2(x_i) + \sum_{i=1}^{N} \sum_{j=1}^{N} (1 - \delta_{ij}) \frac{\partial r}{\partial x_i} \frac{\partial r}{\partial x_j} \sum_{k=1}^{M} b_k(x_i) b_k(x_j) \tag{6}$$

The Kronecker delta can also be used to rewrite the first double summation in Eq. (6). The following identity holds for the first double summation:

$$\sum_{i=1}^{N} \left(\frac{\partial r}{\partial x_i} \right)^2 \sum_{k=1}^{M} b_k^2(x_i) = \sum_{i=1}^{N} \sum_{j=1}^{N} \delta_{ij} \frac{\partial r}{\partial x_i} \frac{\partial r}{\partial x_j} \sum_{k=1}^{M} b_k(x_i) b_k(x_j) \tag{7}$$

Combining Eqs. (6) and (7), we get

$$B^2(r) = \sum_{i=1}^{N} \sum_{j=1}^{N} \delta_{ij} \frac{\partial r}{\partial x_i} \frac{\partial r}{\partial x_j} \sum_{k=1}^{M} b_k(x_i) b_k(x_j) + \sum_{i=1}^{N} \sum_{j=1}^{N} (1 - \delta_{ij}) \frac{\partial r}{\partial x_i} \frac{\partial r}{\partial x_j} \sum_{k=1}^{M} b_k(x_i) b_k(x_j) \tag{8}$$

Simplifying the right-hand side of Eq. (8), we get

$$B^2(r) = \sum_{i=1}^{N} \sum_{j=1}^{N} \frac{\partial r}{\partial x_i} \frac{\partial r}{\partial x_j} \sum_{k=1}^{M} b_k(x_i) b_k(x_j) \tag{9}$$

Partial derivatives in Eq. (9) do not depend on summation index k. Therefore, it is possible to move the summation over k in front of the summations over i and j. We get

$$B^2(r) = \sum_{k=1}^{M} \sum_{i=1}^{N} \sum_{j=1}^{N} \frac{\partial r}{\partial x_i} \frac{\partial r}{\partial x_j} b_k(x_i) b_k(x_j) \tag{10}$$

The second and third summation in Eq. (10) can be written as the product of two summations. Then, we get

$$\sum_{i=1}^{N} \sum_{j=1}^{N} \frac{\partial r}{\partial x_i} \frac{\partial r}{\partial x_j} b_k(x_i) b_k(x_j) = \left[\sum_{i=1}^{N} \frac{\partial r}{\partial x_i} b_k(x_i) \right] \cdot \left[\sum_{j=1}^{N} \frac{\partial r}{\partial x_j} b_k(x_j) \right] \tag{11}$$

We also know that summations on the right-hand side of Eq. (11) only differ in the summation index. Therefore, we get

$$\sum_{i=1}^{N} \frac{\partial r}{\partial x_i} b_k(x_i) = \sum_{j=1}^{N} \frac{\partial r}{\partial x_j} b_k(x_j) \tag{12}$$

Combining Eq. (11) and Eq. (12), we get

$$\sum_{i=1}^{N} \sum_{j=1}^{N} \frac{\partial r}{\partial x_i} \frac{\partial r}{\partial x_j} b_k(x_i) b_k(x_j) = \left[\sum_{i=1}^{N} \frac{\partial r}{\partial x_i} b_k(x_i) \right]^2 \tag{13}$$

Combining Eq. (13) with Eq. (10), we get the formula

$$B^2(r) = \sum_{k=1}^{M} \left[\sum_{i=1}^{N} \frac{\partial r}{\partial x_i} b_k(x_i) \right]^2 \tag{14}$$

Finally, after taking the square root on both sides of Eq. (14), we get for the systematic uncertainty of the result:

$$B(r) = \sqrt{\left[\sum_{i=1}^{N} \frac{\partial r}{\partial x_i} b_1(x_i) \right]^2 + \cdots + \left[\sum_{i=1}^{N} \frac{\partial r}{\partial x_i} b_M(x_i) \right]^2} \tag{15}$$

Meyn interprets Eq. (15) as the Euclidean norm[4] of the systematic uncertainty vector $\boldsymbol{B}(r)$ of the result assuming that a unit uncertainty vector $\boldsymbol{e}_k$ for each independent error source $1 \leq k \leq M$ exists. He writes the systematic uncertainty vector of the result as

$$\boldsymbol{B}(r) = \sum_{k=1}^{M} \left[\sum_{i=1}^{N} \frac{\partial r}{\partial x_i} b_k(x_i) \right] \cdot \boldsymbol{e}_k \tag{16a}$$

where components of the unit uncertainty vector are defined as

$$e_k(\xi) = \begin{cases} 1 & \text{for} \quad \xi = k \quad \text{and} \quad 1 \leq \xi \leq M \\ 0 & \text{for} \quad \xi \neq k \quad \text{and} \quad 1 \leq \xi \leq M \end{cases} \tag{16b}$$

Switching the order of summation in Eq. (16a), we get

$$\boldsymbol{B}(r) = \sum_{i=1}^{N} \sum_{k=1}^{M} \frac{\partial r}{\partial x_i} b_k(x_i) \cdot \boldsymbol{e}_k \tag{17}$$

Partial derivatives of the result are independent of summation index k and therefore can be moved in between both summations. Then, we get

$$\boldsymbol{B}(r) = \sum_{i=1}^{N} \frac{\partial r}{\partial x_i} \cdot \sum_{k=1}^{M} b_k(x_i) \cdot \boldsymbol{e}_k \tag{18}$$

Meyn interprets the second summation in Eq. (18) as the systematic uncertainty vector $\boldsymbol{B}(x_i)$ of a measured variable x_i that lies in the vector space defined by the set of unit uncertainty vectors $\boldsymbol{e}_1, \ldots, \boldsymbol{e}_M$ [see Ref. 3, Eqs. (6) and (7)]. Thus, we can write

$$\boldsymbol{B}(x_i) = \sum_{k=1}^{M} b_k(x_i) \cdot \boldsymbol{e}_k = \begin{bmatrix} b_1(x_i) \\ b_2(x_i) \\ \vdots \\ b_M(x_i) \end{bmatrix} \tag{19}$$

Finally, combining Eqs. (18) and (19), we get Meyn's uncertainty propagation law

$$\boldsymbol{B}(r) = \sum_{i=1}^{N} \frac{\partial r}{\partial x_i} \cdot \boldsymbol{B}(x_i) = \begin{bmatrix} b_1(r) \\ b_2(r) \\ \vdots \\ b_M(r) \end{bmatrix} \tag{20}$$

The systematic uncertainty of the result can now be computed by simply taking the Euclidean norm of the uncertainty vector $\boldsymbol{B}(r)$. Then, we get

$$B(r) = \|\boldsymbol{B}(r)\| = \sqrt{b_1^2(r) + \cdots + b_k^2(r) + \cdots + b_M^2(r)} \quad (21a)$$

$$b_k(r) = \sum_{i=1}^{N} \frac{\partial r}{\partial x_i} \cdot b_k(x_i), \qquad 1 \le k \le M \quad (21b)$$

Meyn's methodology [Eqs. (21a) and (21b)] uses equations that are much simpler than equations used in the mathematically identical traditional methodology [Eqs. (3a–3c)]. No covariance matrix is needed in Meyn's approach, which makes complex uncertainty correlations much easier to understand.

Precision Uncertainty

A precision uncertainty vector can be defined by extending Meyn's original idea to precision uncertainties. In general, assuming that precision uncertainties are not correlated we get the following formula[2]:

$$P(r) = \sqrt{\left[\frac{\partial r}{\partial x_1} P(x_1)\right]^2 + \cdots + \left[\frac{\partial r}{\partial x_N} P(x_N)\right]^2} \quad (22)$$

Equation (22), similar to Eq. (15), can be interpreted as the Euclidean norm of a precision uncertainty vector $\boldsymbol{P}(r)$ assuming that a unit uncertainty vector $\boldsymbol{e}_i$ for each independent measurement $1 \le i \le N$ exists. Components of $\boldsymbol{e}_i$ may be defined as

$$e_i(\mu) = \begin{cases} 1 & \text{for} \quad \mu = i \quad \text{and} \quad 1 \le \mu \le N \\ 0 & \text{for} \quad \mu \ne i \quad \text{and} \quad 1 \le \mu \le N \end{cases} \quad (23)$$

The precision uncertainty vector can then be defined as

$$\boldsymbol{P}(r) = \sum_{i=1}^{N} \frac{\partial r}{\partial x_i} P(x_i) \cdot \boldsymbol{e}_i = \begin{bmatrix} p_1(r) \\ p_2(r) \\ \vdots \\ p_N(r) \end{bmatrix} \quad (24)$$

The precision uncertainty of the result can now be computed by simply taking the Euclidean norm of the precision uncertainty vector $\boldsymbol{P}(r)$. Then, we get

$$P(r) = \|\boldsymbol{P}(r)\| = \sqrt{p_1^2(r) + \cdots + p_i^2(r) + \cdots + p_N^2(r)} \quad (25a)$$

$$p_i(r) = \frac{\partial r}{\partial x_i} \cdot P(x_i), \qquad 1 \le i \le N \quad (25b)$$

Total Uncertainty

Finally, after taking the square root on both sides of Eq. (2) and substituting the systematic and precision uncertainty by using Eqs. (21a) and (25a), we get the following formula for the total uncertainty of the result:

$$U(r) = \sqrt{\|\boldsymbol{B}(r)\|^2 + \|\boldsymbol{P}(r)\|^2} \quad (26)$$

Partial derivatives of the result $r(x_1, \ldots, x_N)$ with respect to measured variables $x_1, \ldots, x_N$ are needed in order to estimate test data uncertainty. The calculation of these derivatives has to be fast, accurate, and reliable in order to meet requirements of an automated near–time uncertainty analysis system for wind-tunnel test data. The forward/backward difference formula can be used to determine partial derivatives. The forward difference approximation of the partial derivative, for example, is given as

$$\frac{\partial r}{\partial x_i} \approx \frac{r(\ldots, x_i + \Delta x, \ldots) - r(\ldots, x_i, \ldots)}{\Delta x} \quad (27)$$

The forward/backward difference formula is fast as only one additional calculation of the result for each independent variable has to be performed. Studies, however, show that the accuracy of the forward/backward difference formula is influenced by the round-off error in the step size Δx. The step size Δx has to be selected such that x_i and $x_i \pm \Delta x$ differ by an exactly representable number. An optimal choice for the step size Δx exists that is given by the formula[5]

$$\Delta x \approx \lambda \cdot \sqrt{\varepsilon} \quad (28)$$

The absolute value of the measured variable itself, that is, $|x_i|$, is often a good choice for the characteristic scale. However, numerical difficulties arise if $|x_i|$ is close to zero. Then, a fraction of the range R_i of the measured variable x_i should be used (e.g., 1%). Finally, the determination of the characteristic scale can be summarized in the formula

$$\lambda = \max[|x_i|;\ R_i \times 0.01] \quad (29)$$

The relative machine precision at run time can be computed using the algorithm given in Ref. 4. This algorithm computes an approximate value for the smallest quantity such that $(1 + \varepsilon) > 1$ in floating point arithmetic.

Numerical studies performed by the author have shown that the forward/backward difference formula in combination with the automatically determined optimum step size provides a sufficiently accurate approximation of the partial derivative for the purpose of estimating wind-tunnel test data uncertainty.

Uncertainty Analysis Algorithm

Key elements of an uncertainty analysis algorithm for wind-tunnel test data were developed in the preceding section. The algorithm can be summarized as follows:

1) Determine partial derivatives $\partial r/\partial x_1, \ldots, \partial r/\partial x_N$ of the result $r(x_1, \ldots, x_N)$ using the forward/backward difference formula.

2) Determine components of systematic uncertainty vectors $\boldsymbol{B}(x_1), \ldots, \boldsymbol{B}(x_N)$ for each measured variable $x_1, \ldots, x_N$.

3) Determine components of the systematic uncertainty vector $\boldsymbol{B}(r)$ by applying Meyn's uncertainty propagation law.

4) Determine components of the precision uncertainty vector $\boldsymbol{P}(r)$ using partial derivatives and precision uncertainty estimates for each measured variable $x_1, \ldots, x_N$.

5) Determine the total uncertainty $U(r)$ of the result by taking the square root of the sum of the squares of the Euclidean norm of the systematic uncertainty vector $\boldsymbol{B}(r)$ and of the precision uncertainty vector $\boldsymbol{P}(r)$.

Summary

Meyn's uncertainty analysis methodology was selected for the uncertainty analysis algorithm of NASA Ames wind tunnels. His approach greatly simplifies the calculation of the systematic uncertainty of a result as it is easier to understand than the mathematically identical traditional methodology. A new derivation of Meyn's uncertainty propagation law was presented in order to gain confidence in his methodology. In addition, Meyn's vector approach was extended to the calculation of the precision uncertainty of a result in order to have a consistent set of equations for the uncertainty analysis of test data.

The successful application of an uncertainty analysis algorithm depends on the ability to determine partial derivatives of a result with sufficient accuracy and reliability. Therefore, the author implemented the forward/backward difference formula in combination with an automatically determined optimum step size in the uncertainty analysis algorithm of NASA Ames wind tunnels.

Acknowledgments

The work reported in this Technical Note was supported by NASA Ames Research Center under Contract NAS2–98083. The author thanks Larry Meyn of NASA for his helpful comments and suggestions.

References

[1]"Assessment of Experimental Uncertainty with Application to Wind Tunnel Testing," AIAA Standard S-071A-1999, Revision A of the Standard, AIAA, Reston, VA, 1999, pp. 11–17.

[2]Coleman, H. W., and Steele, W. G., *Experimentation and Uncertainty Analysis for Engineers*, 2nd ed., Wiley, New York, 1999, pp. 83–88, Eqs. (4.2–4.8).

[3]Meyn, L. A., "An Uncertainty Propagation Methodology That Simplifies Uncertainty Analyses," AIAA Paper 2000-0149, Jan. 2000; Eqs. (4–12).

[4]Forsythe, G. E., Malcolm, M. A., and Moler, C. B., *Computer Methods for Mathematical Computations*, Prentice–Hall, Englewood Cliffs, NJ, 1977, pp. 13, 14, 41.

[5]Press, W. H., Teukolsky, S. A., Vetterling, W. T., and Flannery, B. P., *Numerical Recipes in FORTRAN 77*, 2nd ed., Cambridge Univ. Press, Cambridge, England, U.K., 1996, pp. 180–182.

S. K. Aggarwal
Associate Editor

Rapid Scanning of Overheat Ratios Using a Constant Voltage Anemometer

Joseph D. Norris* and Ndaona Chokani†
North Carolina State University, Raleigh, North Carolina 27695

THE requirements of large bandwidth and high spatial resolution have resulted in thermal hot-wire anemometry being the most widely used tool for the measurement of freestream and boundary-layer/shear-layer fluctuations in high-speed flows. When there is also a need to derive the fluctuations in terms of gas dynamic parameters, this measurement task is more challenging because the hot wire has a mixed mode response to both mass flux and total temperature and the hot wire must be operated at multiple overheats. Furthermore, as most high-speed facilities have relatively short run times, it is highly desirable that these multiple overheats are accomplished within a single run to ensure accuracy in the measured data. The two common modes of operating the hot-wire are the constant-current anemometer (CCA) and the constant-temperature anemometer (CTA). More recently the constant voltage anemometer (CVA) has been introduced by Sarma.[1] In comparison to the CCA and CTA, the CVA's advantages include larger bandwidths, lower electronic noise, and higher sensitivity. The CVA-operated hot wire has been used to characterize the evolution of the transitional hypersonic boundary-layer disturbances by Lachowicz et al.[2] and Doggett et al.[3] The fluctuations in a turbulent supersonic boundary layer have also been documented using the CVA by Comte-Bellot and Sarma[4] and Weiss et al.[5]

Walker et al.[6] demonstrated the rapid scanning of multiple overheats in a CTA to resolve the mass flux and total temperature fluctuations in a supersonic flow. The overheat was stepped through eight operating temperatures at a rate of 10 ms/temperature; the temperature was increased from step to step. More recently, Weiss et al.[7] described the application of a CTA with automatic rapid scanning to measure at six overheats over a test time of 120 ms; the scanning was demonstrated for decreasing values of the overheats. The rapid scanning of multiple overheats using a CTA operation is however problematic because of the coupled frequency response and overheat behavior in the CTA. The frequency response of the CTA can be inferred from the following equation[8]:

$$M_{\mathrm{CTA}} = M_{\mathrm{wire}}/(1 + 2a_w R_w G) \tag{1}$$

where a_w and R_w are the overheat and resistance of the hot wire, respectively, G is the transconductance of the CTA, and M_{CTA} and M_{wire} are the time constants of the CTA and the hot wire, respectively. The CTA bridge can be balanced for an optimum bandwidth for only one overheat; thus, when the bridge is adjusted at the lowest overheat, the bridge becomes unstable at higher overheats. On the other hand, when the bridge is balanced at the highest overheat, its bandwidth decreases with decreasing overheat, Eq. (1).[7] Thus with the rapid scanning of multiple overheats in a CTA, the measurements are either obtained over a small range of overheats or with different bandwidths at each overheat.

The CVA is a second-order system, whose expressions for the hardware time constant T_c, natural frequency ω_n, damping ratio ζ, and bandwidth BW are given in Sarma et al.[9]:

$$T_c = \frac{C R_a R_b}{R_2}, \qquad \omega_n = \sqrt{\frac{R_w}{R_2}\frac{2\pi f_t}{T_c}\left(1 + \frac{R_2}{R_d}\right)}$$

$$\zeta = \frac{1}{2}\left[\left(\frac{1}{T_c} + 2\pi f_t \frac{R_w}{R_d}\right) \Bigg/ \sqrt{\frac{R_w}{R_2}\frac{2\pi f_t}{T_c}\left(1 + \frac{R_2}{R_d}\right)}\right]$$

$$BW = \omega_n \sqrt{(1 - 2\zeta^2) + \sqrt{4\zeta^4 - 4\zeta^2 + 2}} \tag{2}$$

where f_t is the gain bandwidth of the operational amplifier in the CVA circuit (Fig. 1) and

$$1/R_2 = 1/(R_a + R_b) + 1/R_d$$

Sarma[10] has theoretically shown, and Kegerise and Spina[11] have experimentally established, that the bandwidth of the CVA does not change with overheat. This constant bandwidth feature of the CVA coupled with its demonstrated attributes of large bandwidth, low electronic noise, and high sensitivity make it extremely attractive for obtaining calibrated measurements in short-run-time, high-speed facilities. In all of the aforementioned CVA applications,[2–5,9] continuous running high-speed facilities were used. In the present Note we demonstrate the application of the CVA in a short-run-time supersonic wind-tunnel facility.

The associated circuit of the Tao Systems® Model VC-01 CVA used in the present work is shown in Fig. 1. The wire voltage V_w is given in Ref. 10 as

$$V_w = (R_F/R_1)V_1 \tag{3}$$

In the present work a programmable Wavetek® arbitrary waveform generator is used to vary V_1 (and thus V_w and a_w) in six stepped increments with a duration of 20-ms/wire voltage (Fig. 2). A Nicolet®

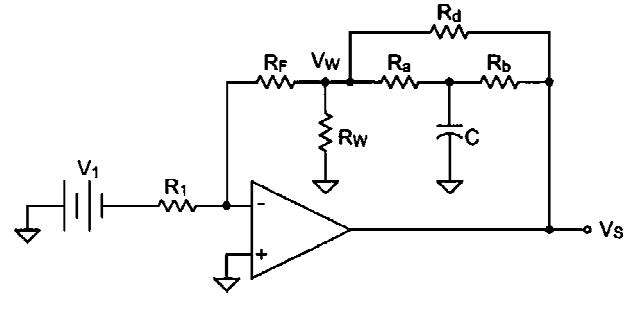

Fig. 1 Compensated CVA circuit (from Ref. 10).

Received 14 October 2002; revision received 10 February 2003; accepted for publication 17 February 2003.

*Research Assistant, Department of Mechanical and Aerospace Engineering; currently Aerospace Engineer, Sverdrup Corporation, Silver Spring, MD 20903. Student Member AIAA.

†Professor, Department of Mechanical and Aerospace Engineering. Associate Fellow AIAA.